ISSN 2706-655X Vol. 7, Issue 3: 111-125, DOI: 10.25236/IJFET.2025.070315

Impact of Position Choosing in the Calculation of Lifting Line Theory

Haoyang Yu

Department of Aeronautical and Aviation Engineering, The Hong Kong Polytechnic University, Hong Kong, China
22101598d@connect.polyu.hk

Abstract: *This investigation examines the critical influence of spanwise position selection on computational accuracy and solution stability in Lifting Line Theory Fourier series representations for finite wing analysis. Lifting Line Theory serves as a fundamental aerodynamic tool for estimating essential performance parameters of the finite wing, including lift coefficient and induced drag, particularly valuable during preliminary wing design phases where computational efficiency takes precedence over detailed flow modeling. The result accuracy and convergent behavior of Lifting Line Theory solutions demonstrate pronounced sensitivity to the placement of spanwise evaluation points within the Fourier series framework. This study systematically evaluates multiple position distribution strategies, encompassing concentrated arrangements near the wing tip and wing root, as well as uniform distributions, to quantify their respective impacts on solution precision and convergence characteristics. The analysis employs tapered wing configurations with symmetric airfoil sections across taper ratios of 0, 0.5, and 1.0, with an aspect ratio of 10. Results demonstrate that specific position angle ranges yield optimal computational accuracy, with substantial error occurring when two varying angular positions both approach either minimal or maximal domain boundaries. The uniform angle distribution methodology ensures robust solution stability and accuracy, even when extending the analysis to high-order term representations exceeding 1000 terms. Alternative distribution schemes exhibit inferior convergence properties and limited stability regions. These findings provide practical guidance for optimal position selection in Lifting Line Theory implementations.*

Keywords: *Lifting Line Theory, Aerodynamics, Fourier Series, Spanwise Position Optimization, Solution Convergence*

1. Introduction

The Lifting Line Theory (LLT) has been an essential part of aerodynamic analysis, providing a straightforward yet powerful method for determining the lift distribution on finite wings. Although considered a fundamental approach, LLT plays a crucial role in estimating vital aerodynamic coefficients such as the wing lift coefficient, induced drag coefficient, lift curve slope, and efficiency factors for both lift and drag. This theory's value becomes evident in the initial design stages of aircraft wings, where more advanced techniques like Computational Fluid Dynamics (CFD) are either computationally expensive or impractical due to time constraints. LLT allows engineers to perform quick evaluations of wing configurations, facilitating faster iterations and reducing the need for complex calculations during early-stage design processes. Despite its benefits, the accuracy of LLT depends heavily on how it is applied, particularly when the Fourier series is used to describe the circulation distribution along the wing span.

Proposed by Prandtl in 1918, the lifting line theory has had several variations in later years. The Fourier series formulation of LLT, introduced by Glauert (1926) [1], simplifies the equations governing the wing's aerodynamics by breaking them into a series of harmonics. This method reduces the complexity of solving the equations, turning them into a set of manageable algebraic expressions. In the equation, the angle θ represents the position on the wing. The distance from the wing root y_{root} for a half span of the wing is related to the angle θ by the equation 1;

$$y_{root} = \frac{b}{2}\cos(\theta) \tag{1}$$

The Fourier series form of LLT, as described by Anderson (2001) [2], is as following equation 2:

ISSN 2706-655X Vol. 7, Issue 3: 111-125, DOI: 10.25236/IJFET.2025.070315

$$\alpha(\theta) = \frac{4b}{a_0 c(\theta)} \sum_{n=1}^{N} A_n \sin n\theta + \alpha_{(L=0)}(\theta) + \sum_{n=1}^{N} n A_n \frac{\sin n\theta}{\sin \theta} \quad (2)$$

In this equation, α(θ) represents the geometric angle of attack at the spanwise position θ, b is the whole span of the wing, a0 is the 2D airfoil lift-curve slope, c(θ) is the chord length at position θ, A_n represents the Fourier coefficients, αL=0(θ) is the zero-lift angle of attack at position θ.

The Fourier coefficients A_n are determined by choosing N positions along the wing span to set up a system of N equations, with each corresponding to an angle θ. The way these positions are selected is critical as they directly affect the accuracy and convergence of the solution. If poorly chosen, the positions can lead to wrong results.

Although the Lifting Line Theory has been extensively applied to various aerodynamic problems, there is a lack of comprehensive studies on how the selection of spanwise positions impacts the accuracy of the Fourier series solution. This article aims to fill this gap by providing detailed guidelines for choosing optimal positions in Fourier series calculations. Specifically, this paper will address:

1) The optimal method for selecting positions in a 4-term Fourier series calculation to achieve accurate results.

2) The effect of varying position distributions on the convergence behavior and accuracy of the calculated results in different scenarios.

3) A certain position distribution for calculating the accurate result converged with the number of terms used in the Fourier series

By addressing these issues, this study will provide valuable insights into how to improve the application of LLT, enhancing both its accuracy and efficiency.

2. Related Work

Prandtl's pioneering work on the LLT in the early 20th century shed insight into the efficiency estimation of the finite wing. Instead of fading into obsolescence, LLT has continued to prove itself as a valuable and versatile tool for current aerodynamic research, helping to predict the optimal design in a variety of fields and applications.

Although the original LLT was only applicable to wings with no sweep, no dihedral, and a high aspect ratio, nowadays, researchers have proposed LLT for complex wing geometries. As proposed by Phillips and Snyder [3], improved by Reid and Hunsaker [4], and finalized by Goates and Hunsaker [5], the modern version of LLT can be applied to a wing with arbitrary sweep, dihedral, and twist. This LLT can predict the efficiency of most wing configurations and can even be applied to wings with wingtips and winglets for design optimization.

Apart from wings, LLT can also be used for wind turbine blade design. The LLT was also utilized within the actuator line model (ALM), which in turn is a numerical tool for describing lifting surfaces, such as wind turbine blades, in CFD calculations. Recent research attempted to reformulate LLT to more accurately capture the ALM, whose approximation error is related to the accumulation of shed vorticity from finite span lifting surfaces, and generalized it to handle drastic changes in chord down the blade [6].

LLT has also been extended to unsteady aerodynamic and aeroelastic analysis. An unsteady lifting-line theory for camber morphing wings was introduced in 2018 by linking an unsteady lifting-line formulation with the Boutet and Dimitriadis aerodynamic theory for state-space aeroelastic modeling [7].

Most of the research relating to LLT, especially studies of the modern LLT, has raised the concern of how to choose the position distribution of the control points or the horseshoe vortex when applying the theory. The cosine clustering was proved to be efficient when applying the modern LLT. According to Phillips and Snyder [3], the straight wing can directly use the cosine clustering on the whole wing, having position concentration at the wingtip. However, since the theory was also designed for the swept wing, the slope of the chord line has a steep change at the root. As a result, the cosine cluster was used on each semispan, which led to concentration on both the wing tip and the wing root and formed a symmetric cosine clustering. The control point distribution is given by:

$$\frac{s_i}{b} = \frac{1}{4}\{1 - cos[\left(\frac{i\pi}{n}\right) - (\frac{\pi}{2n})]\}, \quad 1 \le i \le n$$

With s being the distance from the wing root to the control point, n being the total number of control points on a semispan. The optimal number of control points was proved to be 40 per half span.

ISSN 2706-655X Vol. 7, Issue 3: 111-125, DOI: 10.25236/IJFET.2025.070315

Therefore, cosine clustering may also be beneficial in the Fourier series form of LLT.

3. Methodology

To evaluate the accuracy, the result of the wing's induced drag efficiency factor was examined. The induced drag efficiency factor δ is a factor adding to the minimum induced drag coefficient calculated from the elliptical wing ($\frac{CL^2}{\pi AR}$). The calculation of the induced drag efficiency factor is given below in equation 3;

$$C_{D,i} = \frac{C_L^2}{\pi AR}(1 + \delta) \tag{3}$$

$$where\ \delta = \sum_{2}^{N} n(A_n/A_1)^2$$

The results were obtained by using tapered wings with a symmetric airfoil and without geometric and aerodynamic twists. In equation 1, the 2D airfoil lift-curve slope a_0 is assumed to be 2π, and the angle of attack at zero lift $\alpha_{l=0}(\theta)$ is zero for any θ due to the symmetric airfoil used.

The first term at the right of the equation 1 which includes the wing span b and the local chord length $c(\theta)$ at certain position θ can relate to the aspect ratio AR and taper ratio λ (the chord length at tip divided by the chord length at the root) by the following equation 4:

$$\frac{4b}{a_0 c(\theta)} = \frac{(1+\lambda)AR}{\pi[(\lambda-1)\cos(\theta)+1]} \tag{4}$$

Matrix calculation is used to solve the N equations. If $\{A\}$ is the matrix containing the coefficient of A_n, X is the solution matrix of A_n, and B is the column vector of the angle of attack, then there is $\{A\}[X] = [B]$. Since there is no geometric twist, the angle of attack is constant. This equation can be further rearranged into $\frac{[X]}{\alpha} = \frac{\{reverse\ A\}[B]}{\alpha}$, with $\frac{[B]}{\alpha}$ being the column vector of 1. $\frac{[X]}{\alpha}$ can be directly used to calculate the factor because the calculation only contains the division from of A_n which is $\left(\frac{A_1}{A_n}\right)$. Therefore, the result is independent of the angle of attack.

Two Python programs were used to achieve the three objectives described in the introduction. The first program is to draw the 3D plot indicating how the choosing of two out of four positions affects the result of the 4-term Fourier series. The 4-term Fourier series needs to apply four positions to form four equations, two of which are beforehand defined as the commonly used angles, such as $\frac{\pi}{2}$ and $\frac{\pi}{3}$. The other two positions were traded as two variables that range from 0 to $\frac{\pi}{2}$ uniformly with a number of 50.

The second program is to examine the convergent behavior of the results when applying different position distributions. The maximum number of terms to calculate, the aspect ratio, and the taper ratio of the wing are input to the program. Then the program will give the scatter plot indicating each result of the induced drag efficiency factor calculated using each term number, which can show how and when the result becomes convergent or divergent as the term number increases.

The position distributions can be divided into three categories, which are tightly arranged in the tip, tightly arranged in the root, and a uniform distribution of distance. The distributions are given by different functions whose independent variable x is proportional to the point number in the sequence, and the dependent variable y ranges from 0 to 1 and is the nondimensional distance from the wing root, which is the distance from the wing root y_{root} divided by the half wing span $\frac{b}{2}$. As shown in Figure 1a, the x values are arranged from 0 to the x value where the corresponding y value is 1 or 0, and the intervals between the adjacent x values are identical and equal to 1 divided by the total term number. The y value is calculated from the function by the corresponding x. Then, the angle θ indicating the position in the Fourier series is computed by the equation $\theta = \arccos(y)$. In this way, when y varies from 0 to 1, the θ from $\frac{\pi}{2}$ to 0, the y_{root} varies from 0 to the half span, and the position moves from the wing root to the tip.

The function of the category tightly arranged in the tip has a greater slope when approaching $y = 0$ which is the wing root, and has a smaller slope when approaching $y = 1$ which is the wing tip. The functions of this category include $y = cos(x)$ ($x = \theta$, uniform angle distribution), $y = x^{\frac{1}{r}}$, $y =$

ISSN 2706-655X Vol. 7, Issue 3: 111-125, DOI: 10.25236/IJFET.2025.070315

$-x^p + 1$, and $y = \frac{1}{f}(-e^x + 1) + 1$ where the constant r, p, and f are three factors that can control the slope of the function in the range of the x. In addition, the factors should all greater than 1. Figure 1b shows these four functions with the factor r=2, p=2, and f=6.

The function's slope of the tightly arranged in the root category is in the opposite way of the tightly arranged in the tip. The functions include $y = x^p$, and $y = \frac{1}{f}(e^x - 1)$. The constants p and f also control the slope of the function. The last category is the uniform distribution of the distance using $y = x$.

In addition, the symmetric cosine distribution, which is identical to the cosine clustering mentioned before in the research of Phillips and Snyder [3], was also tested to check if this distribution is applicable in Fourier series LLT. This distribution has points tightly arranged in both the root and tip, while the middle-span is loosely distributed. The function for the symmetric cosine distribution is given by: $y = \frac{1}{2}\{1 - cos[(x) - (\frac{\pi}{2n})]\}$.

Figure 2a and Figure 2b demonstrate how the position points are distributed on the semispan for different functions. The x-axis of the plot is the nondimensional distance from the wing root. Figure 2a shows the tip concentration and symmetric cosine distribution, while Figure 2b shows the root concentration and uniform distance distribution.

Both programs applied the aspect ratio of 10 and the taper ratio of 0, 0.5, and 1 as examples to examine the result of the wing's induced drag efficiency factor.

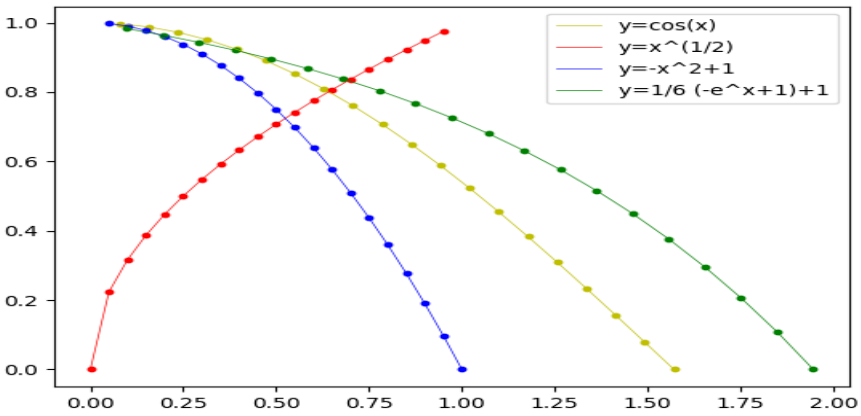

Figure 1a: Functions with Variable Slopes Based on y Value for Tightly Arranged Positions

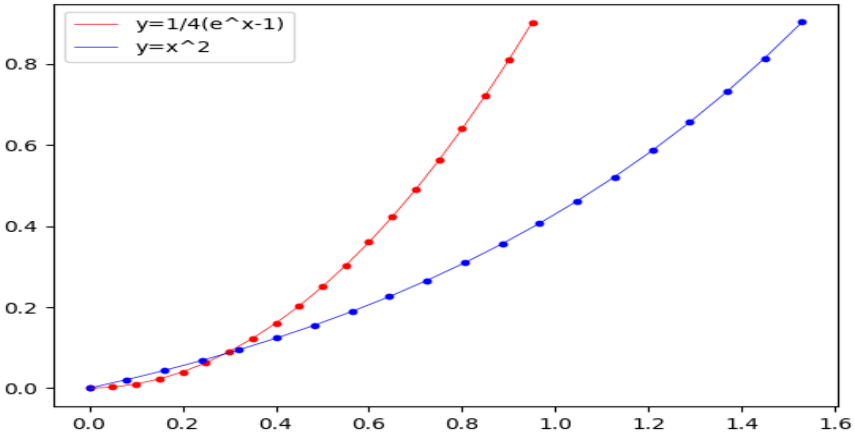

Figure 1b: Functions Representing Slope Behavior for Tightly Arranged in Root Positions

ISSN 2706-655X Vol. 7, Issue 3: 111-125, DOI: 10.25236/IJFET.2025.070315

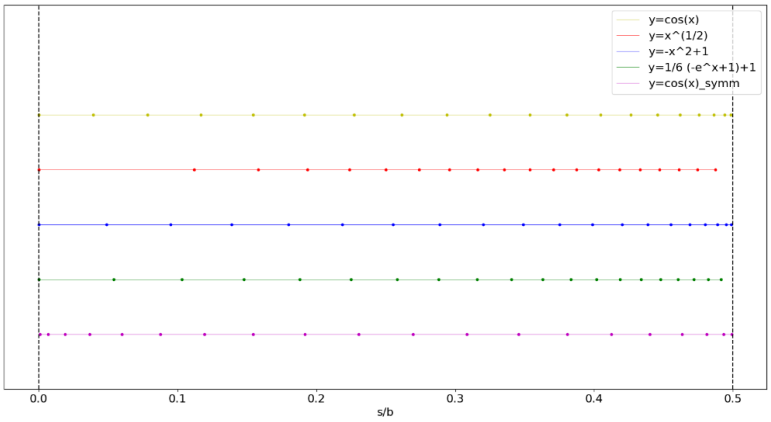

Figure 2a: tip concentration and symmetric cosine distribution

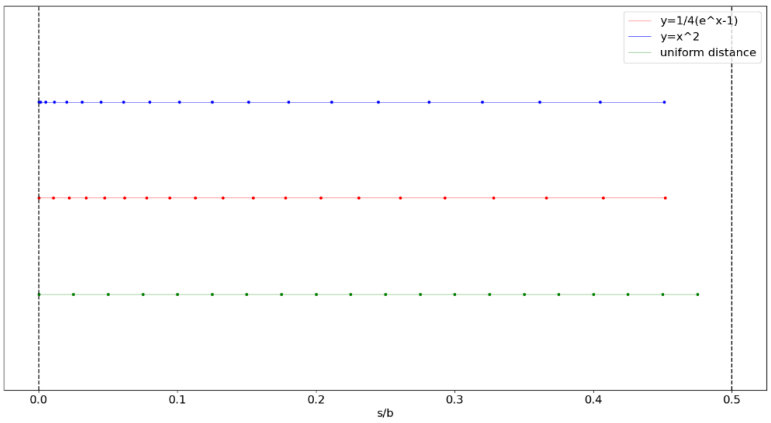

Figure 2b: root concentration and uniform distance distribution

4. Results

4.1 Position choosing for a 4-trem Fourier series

The results derived from applying a 4-term Fourier series using fixed angles of $\pi/2$ and $\pi/3$, along with two varying angles, are presented below. In all the calculations, the aspect ratio (AR) is maintained at 10, and taper ratios are set at 0, 0.5, and 1, as shown in Figures 3a-f.

Figure 3 presents 3D surface plots where the x and y axes represent the two varying spanwise position angles, while the z-axis displays the calculated induced drag efficiency factor (δ). The red points on the plot correspond to the validated reference results from Bridge's study (2005) [8] for each taper ratio at AR = 10. The yellow regions identify areas where the efficiency factor approaches the reference value (δ ≈ reference value ± 0.005). These regions demonstrate that specific configurations of the varying angles align with aerodynamically efficient solutions. The absence of result points along the diagonal line y = x occurs because this condition creates a mathematically singular system where two identical angles reduce the four-equation system to only three independent equations, making the 4-term Fourier series unsolvable. The yellow regions reveal critical patterns in position selection to obtain an accurate result: First, significant deviations from accurate results occur when both varying angles are very large or very small, either both approaching zero or both approaching π/2. The results may not be accurate when selecting values at the right side of the line $y = -x + 2.1$. Second, the patterns support the observation that when one angle lies within the range 0.3 to 0.4 and the companion angle falls between 0.9 and 1.3, the results are mostly accurate in these three different taper ratio cases so this range may have a greater chance of generating accurate results. These angular ranges ensure balanced representation of root, mid-

ISSN 2706-655X Vol. 7, Issue 3: 111-125, DOI: 10.25236/IJFET.2025.070315

span, and tip flow physics so that accurate results can be generated.

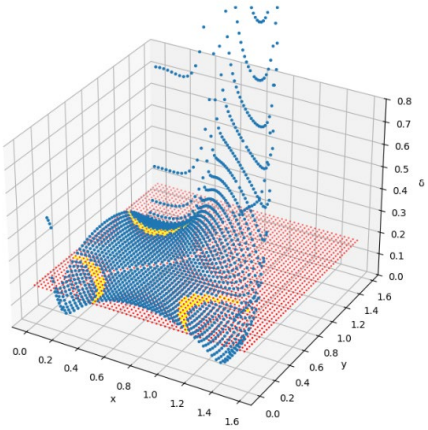

Figure 3a: 3D Surface Plot for 0 taper ratio

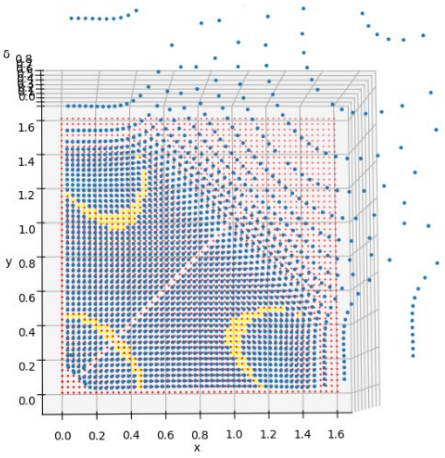

Figure 3b: Top view of 3D Surface Plot for 0 taper ratio

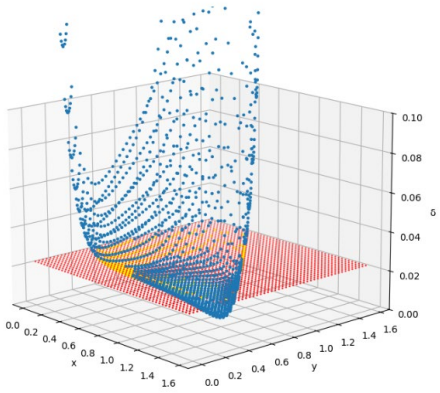

Figure 3c: 3D Surface Plot for 0.5 taper ratio

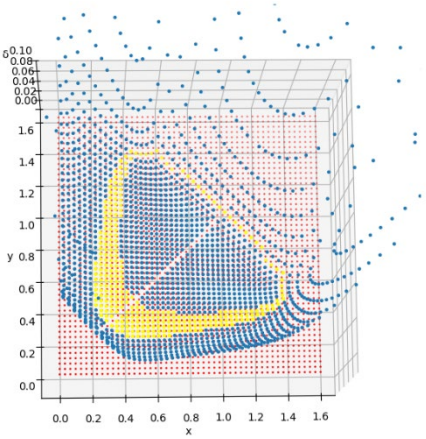

Figure 3d: Top view of 3D Surface Plot for 0.5 taper ratio

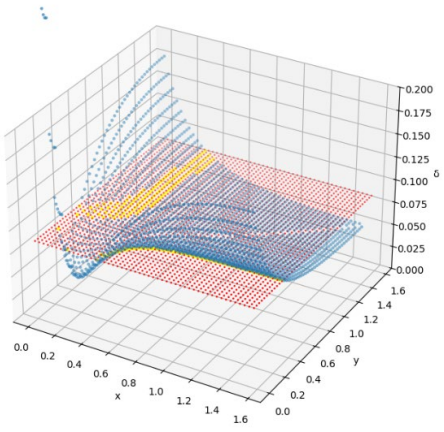

Figure 3e: 3D Surface Plot for 1 taper ratio

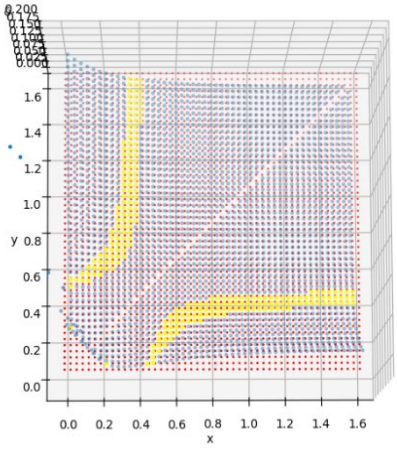

Figure 3f: Top view of 3D Surface Plot for 1 taper ratio

ISSN 2706-655X Vol. 7, Issue 3: 111-125, DOI: 10.25236/IJFET.2025.070315

4.2 Convergent behavior of the results when applying different position distributions

The convergence characteristics of Lifting Line Theory solutions exhibit substantial variation across three primary distribution categories: positions concentrated near the wing tip, positions concentrated near the wing root, and uniform distributions. Analysis reveals that root-concentrated and uniform distance distributions either fail to achieve convergence or produce extremely limited convergent regions, while tip-concentrated distributions demonstrate relatively better convergence properties.

Root-concentrated distributions, characterized by mathematical functions exhibiting shallow gradients near the wing root (y = 0) and steep gradients approaching the tip (y = 1), consistently demonstrate poor convergence behavior. Representative functions include $y = x^p$ and $y = \left(\frac{1}{f}\right)(e^x - 1)$, where parameters p and f control the concentration intensity. Despite systematic parameter optimization, these distributions fail to establish sufficiently robust convergent regions for reliable engineering application.

Figure 4a illustrates the convergence behavior for the $y = x^p$ distribution with p = 2 and taper ratio λ = 1. The results demonstrate convergence initiation around the 10th Fourier term, where calculated efficiency factors approach the theoretical reference value. However, after this convergence zone, the solutions exhibit severe divergence characterized by unrealistically large efficiency factor values. This behavior stems from inadequate sampling of the critical tip region.

Figure 4b presents results for the exponential root-concentrated function $y = \left(\frac{1}{f}\right)(e^x - 1)$ with f = 6 and taper ratio λ = 1. Similar convergence patterns emerge, with solutions stabilizing near the reference value only in a small region before divergence to physically unrealistic magnitudes. The exponential concentration exacerbates the sampling imbalance, providing excessive resolution near the wing root while inadequately representing the aerodynamically critical tip region.

Figure 4c demonstrates the complete convergence failure for the $y = x^p$ distribution when taper ratio reduces to λ = 0 (triangular wing planform). The triangular geometry amplifies the negative effects of root concentration, as the zero chord length at the tip creates additional complexity. The combination of root-concentrated sampling and triangular platform produces persistent divergence without any identifiable convergent region, rendering this approach unsuitable for tapered wing analysis.

Figure 4d shows the exponential root-concentrated distribution performance with taper ratio λ = 0.5 and f = 6. The intermediate taper ratio fails to mitigate the fundamental sampling inadequacy, resulting in continued divergence without convergence establishment. This demonstrates that root-concentrated distributions are inherently incompatible with tapered wing geometries due to their failure to adequately represent tip flow physics.

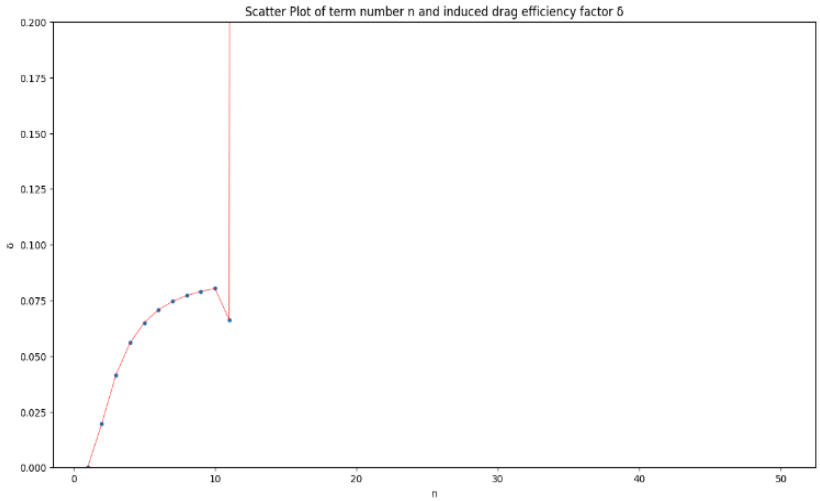

Figure 4 a $y = x^p$ distribution with p=2 and taper ratio=1

ISSN 2706-655X Vol. 7, Issue 3: 111-125, DOI: 10.25236/IJFET.2025.070315

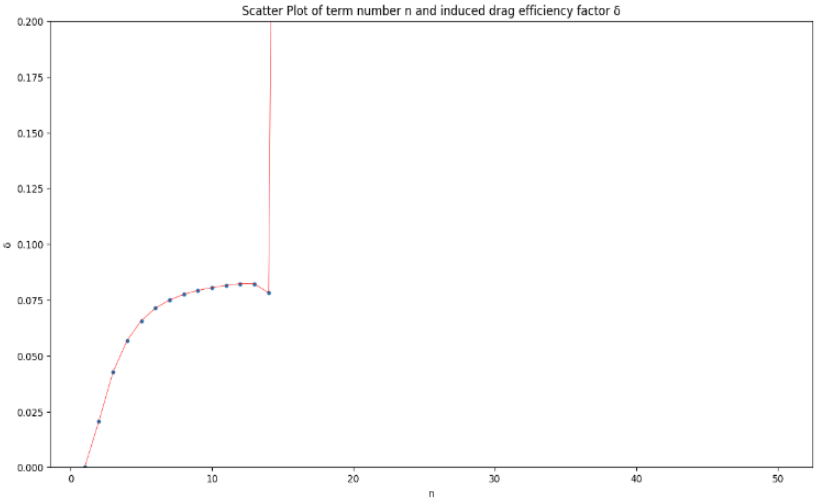

Figure 4 b $y = \frac{1}{f}(e^x - 1)$ *distribution with f=4 and taper ratio=1*

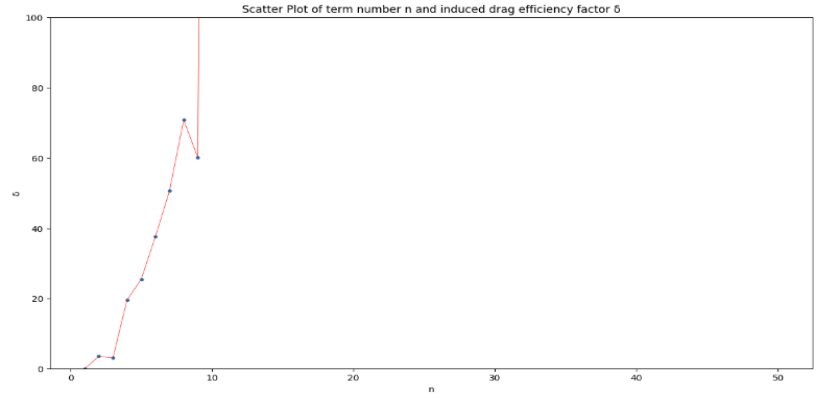

Figure 4 c $y = x^p$ *distribution with p=3 and taper ratio=0*

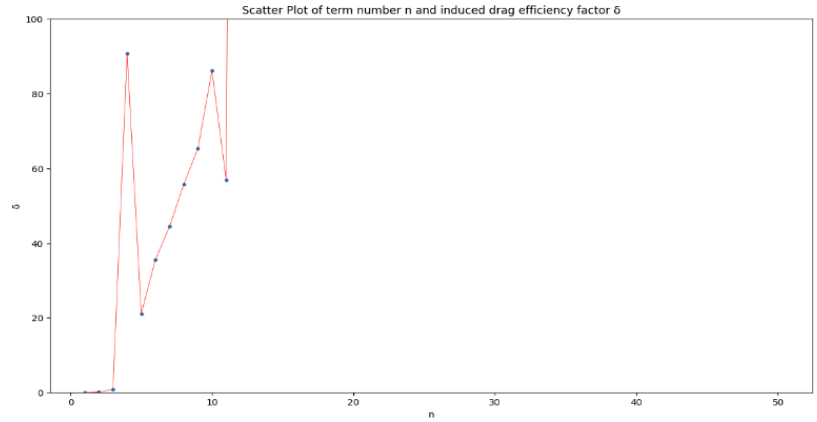

Figure 4 d $y = \frac{1}{f}(e^x - 1)$ *distribution with f=4 and taper ratio=0.5*

For root-concentrated distribution, only when the taper ratio equals 1 among the three ratios, the results become convergent in a small region around the 10th term. As stated by Goates and Hunsaker [5], the vortex shedding happens more intensely near the wingtip. This might be the reason why the root-

ISSN 2706-655X Vol. 7, Issue 3: 111-125, DOI: 10.25236/IJFET.2025.070315

concentrated distribution generated inaccurate results, and more positions sampling should be conducted near the wing tip.

The uniform distance distribution y = x provides equal physical spacing along the wing span. This distribution category exhibits convergence characteristics similar to root-concentrated methods but with marginally improved performance.

Figure 5a presents the uniform distance distribution results for taper ratio λ = 1. The convergence pattern mirrors that observed in root-concentrated distributions, with stabilization around the 10th term. However, the convergent region demonstrates greater stability compared to root-concentrated methods, probably attributed to improved tip region sampling.

Figure 5b illustrates the uniform distance distribution with taper ratio λ = 0.5. No obvious convergent region was shown in the figure, which further supports the idea that taper ratio 1 is more conducive to establishing a convergent region.

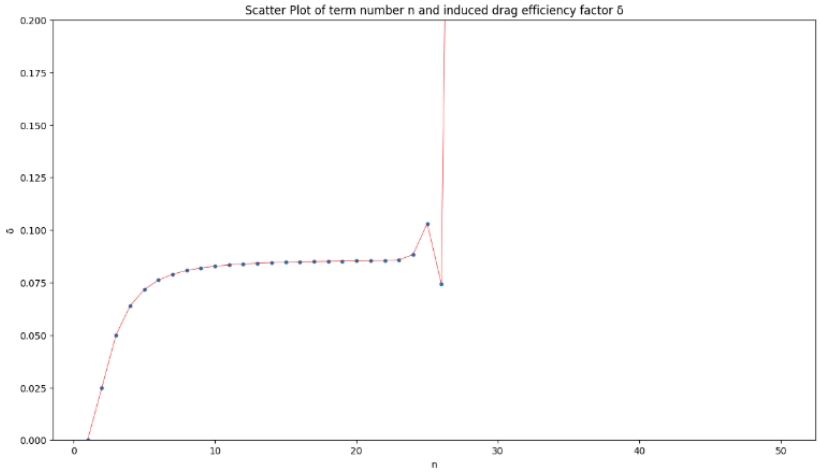

Figure 5 a uniform distance distribution with taper ratio=1

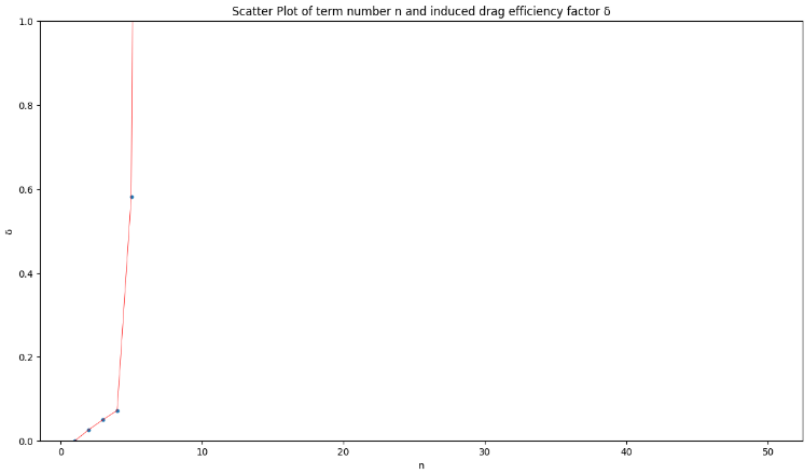

Figure 5 b uniform distance distribution with taper ratio=0.5

The tip-concentrated distribution is more likely to generate a continuously convergent region, providing a certain result. The functions considered in this category include $y = \cos(x)$ $(x = \theta$, uniform angle distribution), $y = x^{\frac{1}{r}}$, $y = -x^p + 1$, and $y = \frac{1}{f}(-e^x + 1) + 1$. Among these, the uniform angle distribution stands out as the only function that ensures the results remain convergent continuously after the term number reaches 1000. Furthermore, the number of terms needed before convergence typically does not exceed 15, making it possible to achieve a result with decent accuracy. If

ISSN 2706-655X Vol. 7, Issue 3: 111-125, DOI: 10.25236/IJFET.2025.070315

the lifting line theory is applied with more than 15 terms for precise results, or 10 terms for close approximations, the uniform angle distribution can be used without the concern of results diverging after reaching convergence.

Figure 6a demonstrates the uniform angular distribution performance with taper ratio $\lambda = 1$. Following a brief initial adjustment within the first few terms, the solution rapidly converges to the theoretical reference value and maintains stability throughout the entire 1000-term analysis range.

Figure 6b shows uniform angular distribution results for the challenging triangular wing case ($\lambda = 0$). Despite the geometric complexity introduced by the triangular platform, the solution maintains convergence stability after initial adjustment. This demonstrates the method's robustness across diverse wing geometries and validates its suitability for general engineering applications. The exceptional stability may result from the uniform angular distribution's preservation of the mathematical orthogonality properties inherent in Fourier series representations. Therefore, the uniform angle distribution can not only prevent generating an ill-conditioned coefficient matrix, but also have adequate sampling near the wing tip. Moreover, the reason for failing to reach a stable convergent result for other distributions (including the other tip-concentrated distribution) might lie in being unable to maintain the discrete orthogonality of the Fourier series, so that the distribution generates an ill-conditioned coefficient matrix, amplifies the error, and generates inaccurate results when solving the matrix X.

Together, Figures 6a and 6b demonstrate that the uniform angle distribution is the most reliable method for ensuring convergence when applying the lifting line theory with more than 15 terms. The results remain stable and approach the reference value with multiple taper ratios, making it a suitable approach for accurate predictions without the risk of divergence.

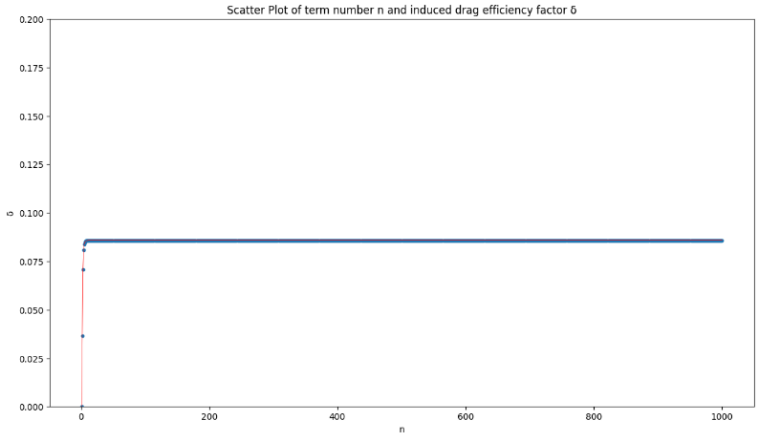

Figure 6 a uniform angle distribution with taper ratio=1

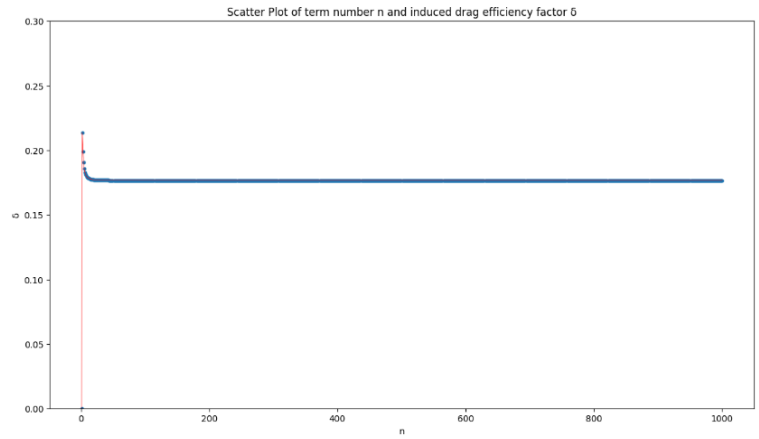

Figure 6 b uniform angle distribution with taper ratio=0

ISSN 2706-655X Vol. 7, Issue 3: 111-125, DOI: 10.25236/IJFET.2025.070315

For other functions in the tip-concentrated distribution category, which includes root functions, negative power functions, and negative exponential functions, the figures below (Figures 7a-g) demonstrate their different convergent behavior.

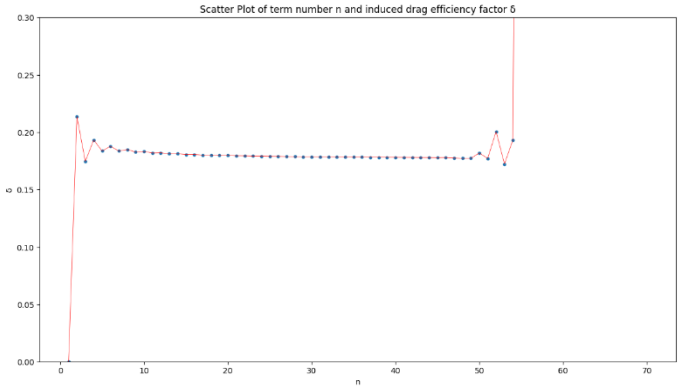

Figure 7 a $y = x^{\frac{1}{r}}$ *distribution with r=2 and taper ratio=0*

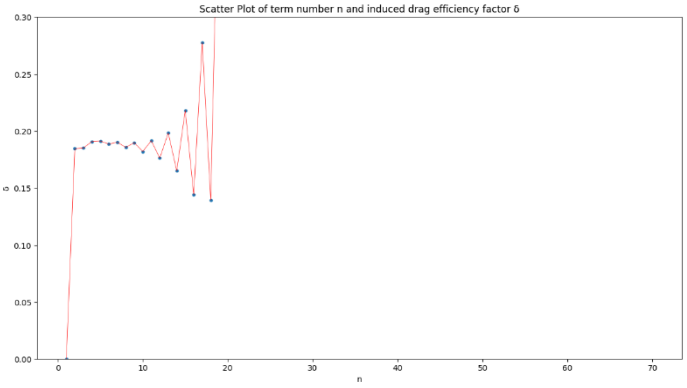

Figure 7 b $y = x^{\frac{1}{r}}$ *distribution with r=3 and taper ratio=0*

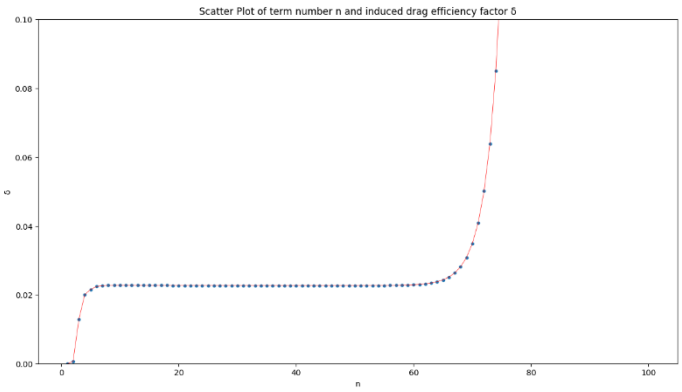

Figure 7 c $y = -x^p + 1$ *distribution with p=2 and taper ratio=0.5*

For the root function $y = x^{\frac{1}{r}}$, when $r = 2$, the results often fluctuate in the first 15 terms, with the amplitude of these fluctuations gradually decreasing as the term number increases, allowing the results to approach a stable result that is close to the reference value. However, after about 50 terms, the results begin to fluctuate again, and the fluctuations grow, eventually causing the results to diverge to very large values.

ISSN 2706-655X Vol. 7, Issue 3: 111-125, DOI: 10.25236/IJFET.2025.070315

However, when increasing or reducing the root factor r, the result is not likely to converge, and it fluctuates around the reference value with a relatively large amplitude, as indicated in Figure 7b.

For the negative power function $y = -x\hat{}p + 1$, when choosing $p = 2$, the result for the three tested taper ratios becomes convergent in a similar manner as the uniform angle distribution, but the results quickly increase and become divergent after 60 to 70 terms, as shown in Figure 7c. When the factor p is greater or less than 2, the results fluctuate around the reference value in the first several terms. The fluctuation becomes more intense as the factor p gets away from 2. Figure 7d. demonstrates the fluctuation when factor p=3 and taper ratio=0.5.

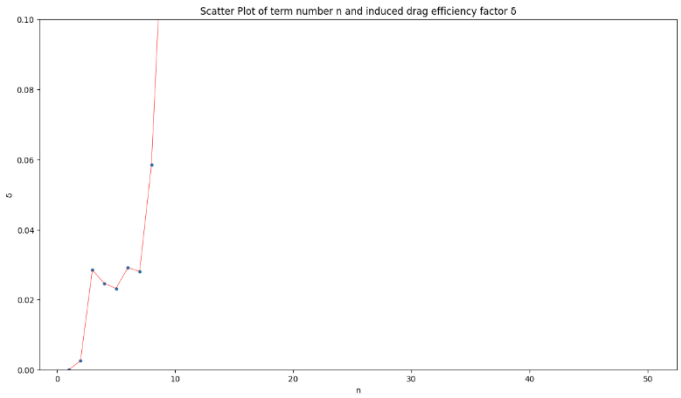

Figure 7 d $y = -x^p + 1$ *distribution with p=3 and taper ratio=0.5*

For the negative exponential function $y = 1/f\ (-e\hat{}x + 1) + 1$, when f is less than 10, the results fluctuate with the fluctuating amplitude decreasing at first and increasing afterward, as shown in Figure 7e. When f reaches 7, a region with steady convergent and accurate results appears, as shown in Figure 7f. When f increases from 7 to 10, the convergent region shrinks, and when the factor f is larger than 10, the convergent region begins to fluctuate, and the results after the convergent region climb to very large values, as demonstrated in Figure 7g, whose factor f equals 15 with the taper ratio as 0.5.

These observations in Figures 7a-g highlight how different tip-concentrated distributions and variations in the parameters *r*, *p*, and *f* influence the convergence and stability of the results. While some values of these parameters, such as *r*=2, *p*=2, or *f*=7, lead to stable convergence, many of the other values cause the results to fluctuate excessively and diverge, preventing long-term stability. The choice of the functions as well as the parameters both play a crucial role in determining whether a function will produce consistent, convergent results or whether it will diverge to large values.

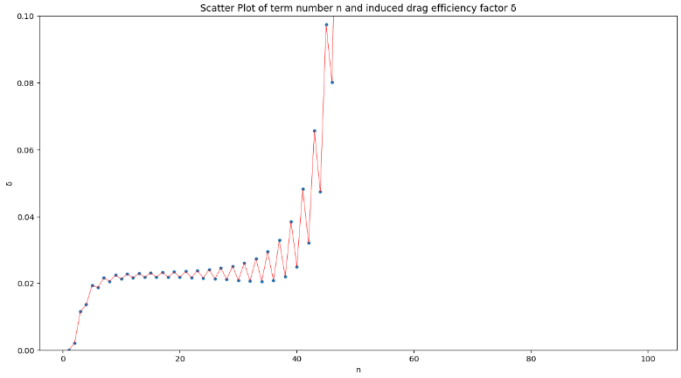

Figure 7 e $y = \frac{1}{f}(-e^x + 1) + 1$ *distribution with f=5 and taper ratio=0*

A supplementary experiment was conducted for the symmetric cosine distribution. The results indicated that this distribution is not as robust as the uniform angle distribution, though these distributions are both related to cosine clustering. As shown in Figure 8a, the results converged to the reference value in a small region and diverged before the 30th term when the taper ratio equals 1. For a taper ratio equal

ISSN 2706-655X Vol. 7, Issue 3: 111-125, DOI: 10.25236/IJFET.2025.070315

to 0.5, as shown in Figure 8b, the results failed to converge, but hovered around the reference value before the 10th term, after which the results diverged. This unalignment between the modern LLT and the current study for whether the symmetric cosine distribution can obtain decent results may be because the modern LLT does not apply the Fourier series form of the LLT.

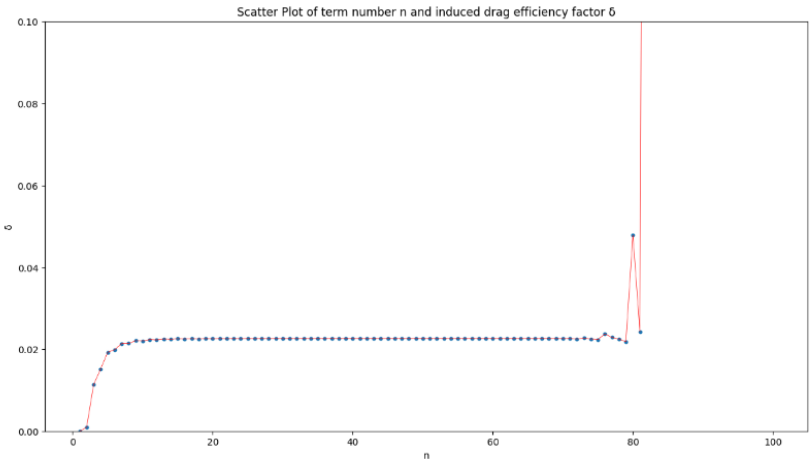

Figure 7 f $y = \frac{1}{f}(-e^x + 1) + 1$ *distribution with f=7 and taper ratio=0.5*

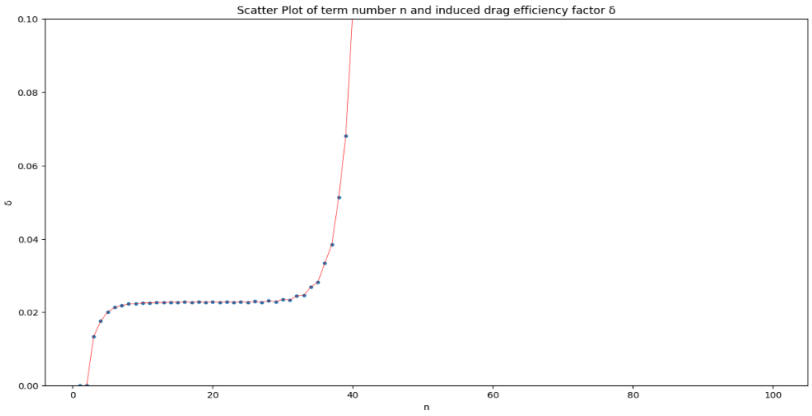

Figure 7 g $y = \frac{1}{f}(-e^x + 1) + 1$ *distribution with f=15 and taper ratio=0.5*

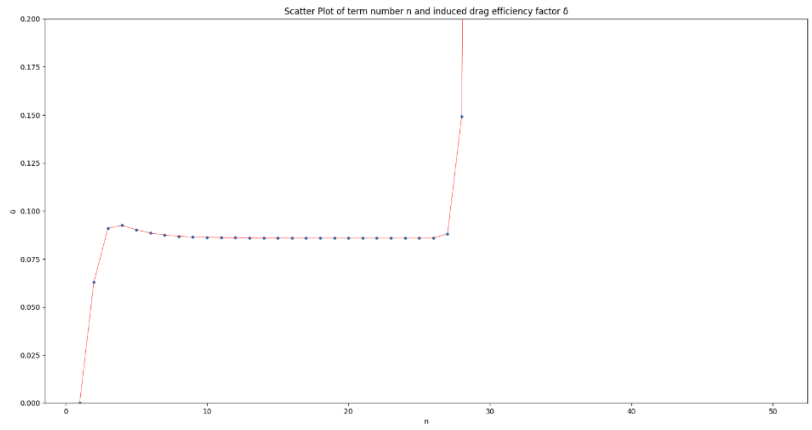

Figure 8 a Symmetric cosine *distribution with taper ratio=1*

ISSN 2706-655X Vol. 7, Issue 3: 111-125, DOI: 10.25236/IJFET.2025.070315

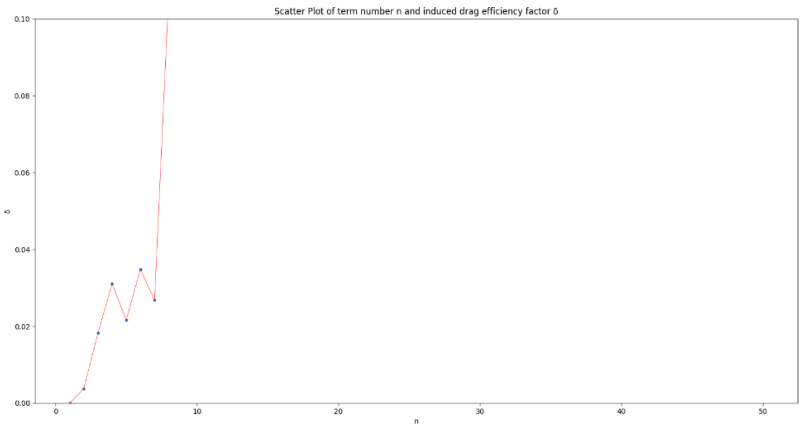

*Figure 8 b S*ymmetric cosine *distribution with taper ratio=0.5*

5. Conclusion

This investigation established the fundamental importance of choosing proper spanwise position selection in determining computational accuracy and solution stability within Lifting Line Theory implementations in Fourier series form. The systematic analysis across different position distributions revealed critical findings that advance the practical application of this classical aerodynamic theory in modern computational environments.

The selection of evaluation points along the wing span emerges as a decisive factor in achieving accurate aerodynamic predictions. For 4-trem Fourier series with two position angles fixed as $\pi/2$ and $\pi/3$, computational experiments demonstrated that substantial solution errors manifest when two varying angles simultaneously approach the same extreme domain boundaries, either both approaching zero or the upper limit of $\pi/2$. Conversely, optimal accuracy consistently emerged when one position angle occupied the range 0.3 to 0.4 radians while the companion angle fell within 0.9 to 1.3 radians. This specific configuration ensures balanced representation of root, mid-span, and tip flow physics while maintaining favorable coefficient matrix conditioning essential for numerical stability across all tested wing geometries.

The distinct convergence behavior for different position distribution categories revealed performance disparities that fundamentally impact the practical utility of Lifting Line Theory applications. Uniform angular distribution methodology emerged as the superior approach, consistently achieving robust and fast convergence across all examined wing geometries and maintaining solution stability throughout extended Fourier series expansions exceeding 1000 terms. This method's exceptional performance stems from its preservation of mathematical orthogonality properties fundamental to Fourier series representations, resulting in well-conditioned coefficient matrices and proper sampling of aerodynamically critical wing regions.

Root-concentrated and uniform distance distributions demonstrated consistently poor convergence characteristics, typically producing either complete divergence or limited convergence windows insufficient for reliable engineering application. Root-concentrated arrangements failed because they oversample regions of gradual circulation change while inadequately representing the critical tip region where vortex shedding is intensive. The uniform distance approach showed marginal improvement over root-concentrated methods with larger convergent regions. These distribution methods become particularly problematic for tapered wing configurations, where taper ratios of 0.5 and 0 consistently prevented convergence establishment.

The practical engineering implications of these findings extend beyond theoretical interest to direct design applications. The identified optimal angle ranges and distribution provide engineers with quantitative criteria for position selection that enhance both computational accuracy and efficiency, offering immediate practical value for aerospace engineers conducting preliminary wing design analysis. The uniform angle distribution method proves particularly valuable for iterative design processes where rapid yet accurate aerodynamic assessment capabilities are essential for efficient configuration evaluation. While this study employed simplified wing geometries characterized by constant taper ratios and

ISSN 2706-655X Vol. 7, Issue 3: 111-125, DOI: 10.25236/IJFET.2025.070315

symmetric airfoils, the research opens pathways for exploring complex wing configurations, including swept planforms.

References

[1] H. Glauert, The Elements of Aerofoil and Airscrew Theory. Cambridge, UK: Cambridge University Press, 1926 (reprinted 1943)
[2] Anderson, J. D., Fundamentals of Aerodynamics, 3rd ed., New York, McGraw-Hill, 2001.
[3] W. F. Phillips and D. O. Snyder, "Modern Adaptation of Prandtl's Classic Lifting-Line Theory," Journal of Aircraft, vol. 37, no. 4, pp. 662-670, 2000, doi: 10.2514/2.2649.
[4] J. T. Reid and D. F. Hunsaker, "A General Approach to Lifting-Line Theory, Applied to Wings with Sweep," Utah State University, Logan, UT, USA, Tech. Rep., 2024.
[5] C. D. Goates and D. F. Hunsaker, "Modern Implementation and Evaluation of Lifting-Line Theory for Complex Geometries," Journal of Aircraft, vol. 60, no. 2, pp. 490-508, 2023.
[6] L. A. Martínez-Tossas and C. Meneveau, "Filtered Lifting Line Theory and Application to the Actuator Line Model," Journal of Fluid Mechanics, vol. 883, pp. 1-27, 2019.
[7] J. Boutet and G. Dimitriadis, "Unsteady Lifting Line Theory Using the Wagner Function for Aerodynamic and Aeroelastic Modelling of 3D Wings," Aerospace, vol. 5, no. 3, Sep. 2018, doi:10.3390/AEROSPACE5030092.
[8] D. Bridges, "Finite wing lift-curve slope calculations using lifting-line theory," 23rd AIAA Applied Aerodynamics Conference, Jun. 2005. doi:10.2514/6.2005-4839